

Testing dispersion of gravitational waves from eccentric sources*

Shu-Cheng Yang,^{1,2} Wen-Biao Han,^{1,2,†} Shuo Xin,³ and Chen Zhang^{1,2}

¹*Shanghai Astronomical Observatory,*

Chinese Academy of Sciences, Shanghai, 200030, China

²*School of Astronomy and Space Science,*

University of Chinese Academy of Sciences, Beijing, 100049, China

³*School of Physics Sciences and Engineering,*

Tongji University, Shanghai 200092, China

(Dated: June 19, 2022)

Abstract

In general relativity, there is no dispersion in gravitational waves, while some modified gravity theories predict dispersion phenomena in the propagation of gravitational waves. In this Letter, we demonstrate that this dispersion will induce an observable deviation of waveforms if the orbits have large eccentricities. The mechanism is that the waveform modes with different frequencies will be emitted at the same time due to the existence of eccentricity. During the propagation, because of the dispersion, the arrival time of different modes will be different, then produce the deviation and dephasing of waveforms compared with general relativity. This kind of dispersion phenomena related with extreme-mass-ratio inspirals could be observed by space-borne detectors, and the constraint of dispersion could be improved three orders of magnitude compared to the current level.

PACS numbers: 04.70.Bw, 04.80.Nn, 95.10.Fh

* This work is supported by NSFC No. U1431120 and No.11273045

† wbhan@shao.ac.cn

Introduction. After one century, the gravitational waves (GWs) which were predicted by Einstein's general relativity, has been detected by advanced LIGO (aLIGO) and advanced Virgo (AdV) in a few of events up to now[1–6]. According to general relativity (GR), GWs with different frequencies propagate at the speed of light c . In other words, GWs are non-dispersive. In theories of quantum gravity, the graviton is the force carrier of gravity, and if GWs are non-dispersive then gravitons are massless. However, in some modified gravity theories[7–10], GWs are dispersive. In these modified gravity theories, the rest mass of graviton is non-zero, and the speed of graviton depends on its frequency(energy). Consequently, the GWs would travel faster or slower than light, and their speed is frequency-related speed.

The signals of GWs emitted from compact binaries belongs to chirp signals, of which the frequency increases over time. If GWs are dispersive and we assume that low-frequency GWs would travel slower, gravitons emitted earlier will also travel slower, leading to a frequency-dependent dephasing of GWs in GR cases.

Usually, researchers use the above physical image to test the dispersion of GWs. While in this Letter we propose a new mechanism which also could be employed to test the dispersion of GWs. In our physical image, one eccentric binary system will emit GWs with varied modes of frequencies at the same moment. It will lead to a more significant dephasing of the GWs in GR cases if GWs are dispersive or equivalently gravitons are massive. Generally speaking, the elliptic orbit of a comparable massive binary will be circularized at the final stage of inspiral(where the GWs are strong enough to be detected), so that the eccentricity of the orbit could be omitted. However, for the large mass-ratio cases such as extreme-mass-ratio inspirals (EMRIs) and intermediate-mass-ratio inspirals (IMRIs), due to the formation mechanism and relatively weak radiation, it is believed that the residual eccentricity could be large at the final stage of inspirals in most cases [11].

In this Letter, based on the physical image we discussed above, we propose that the GWs from eccentric EMRIs/IMRIs could be used to test the dispersion of GWs with higher accuracy compared with the previous methods. Because of the low frequency, this kind of GWs could be detected by space-borne interferometers such as LISA[12], Taiji[13] and TianQin[14].

GW dispersion. The distinct differences between GR and some modified gravity theories located in the dispersion relation. In GR's theory framework, the rest mass of graviton

m_g must be zero like photon or other massless particles, of which the dispersion relation is $E = pc$, where E and p denotes the total energy and momentum of graviton, and c is the speed of light in vacuum. While in some modified gravity theories, m_g could be non-zero. The same as Ref. [15], we consider a Lorentz-violating graviton dispersion relation of the form $E^2 = p^2 c^2 + m_g^2 c^4 + \mathbb{A} p^\alpha c^\alpha$, where α and \mathbb{A} are Lorentz-violating parameters which characterize the difference between GR and modified gravity theories. The values of α and \mathbb{A} are different in different modified gravity theories. The speed of graviton v_g (i.e. the group velocity of GWs) in this dispersion relation is [15]

$$\frac{v_g^2}{c^2} = 1 - \frac{m_g^2 c^4}{E^2} - \mathbb{A} E^{\alpha-2} \left(\frac{v_g}{c} \right)^\alpha. \quad (1)$$

The constraint on m_g play an important role in the dispersion of GWs. In the following, we consider the simplest situation that \mathbb{A} is set to zero, in which there is no violation of Lorentz invariance. In this case, Eq. (1) reduces to that of a simple massive graviton, i.e.

$$\frac{v_g^2}{c^2} = 1 - \frac{m_g^2 c^4}{E^2}. \quad (2)$$

In some astrophysical events such as GW sources with electromagnetic counterparts, we could give a rough constraint on m_g by Eq. (2), providing the information of the ratio of v_g and c . The total energy of graviton E here could be acquired from the frequency f of GWs by de Broglie relations. In 2017, a multi-messenger observation [6, 16] of binary neutron star merger shown a 1.7 s delay of the gamma-ray burst compared to the merger time, and the merge frequency is about 400 Hz. The speed difference between GWs and light in vacuum ($v_g - c$) is from -3×10^{-15} to $+7 \times 10^{-16}$ times the speed of light[17]. By using above data and Eq. (2), we get the constraints on the rest mass of graviton $m_g \leq 1.3 \times 10^{-19}$ eV/ c^2 and the Compton wavelength of graviton $\lambda_g > 9.7 \times 10^9$ km. The accuracy of this estimation on m_g would be better with more such events be detected in future.

Another way to constrain m_g focuses on the gravitational waveform of compact binaries. As mentioned above, if GWs are dispersive, then GWs with different frequencies would propagate in different velocities. During the evolution of compact binaries, the high-frequency GWs produced later would propagate faster than the low-frequency GWs produced earlier. Consequently, there would be distortion applied to the waveforms of GWs compared to that of non-dispersive cases. Considering two gravitons emitted at t_e and t'_e with different frequency f_e and f'_e (or with energies E_e and E'_e), which will be received at corresponding arrival

times t_a and t'_a . Providing during the difference of emitting time ($\Delta t_e = t_e - t'_e$) there is little change on the scale factor a , then the delay of arrival times of two gravitons ($\Delta t_a = t_a - t'_a$) is [15, 18]

$$\Delta t_a = (1 + Z) \left[\Delta t_e + \frac{cD}{2\lambda_g^2} \left(\frac{1}{f_e^2} - \frac{1}{f_e'^2} \right) \right], \quad (3)$$

where Z is the cosmological redshift, and

$$D = \frac{c(1 + Z)}{a_0} \int_{t_e}^{t_a} a(t) dt, \quad (4)$$

where $a_0 = 1$ is the present value of the scale factor. For our accelerating universe [19] that is dominated by dark energy, D and the luminosity distance D_L have the forms [15, 18]

$$D = \frac{c(1 + Z)}{H_0} \int_0^Z \frac{(1 + z')^{-2} dz'}{\sqrt{\Omega_M(1 + z')^3 + \Omega_\Lambda}} \quad (5)$$

and

$$D_L = \frac{c(1 + Z)}{H_0} \int_0^Z \frac{dz'}{\sqrt{\Omega_M(1 + z')^3 + \Omega_\Lambda}}, \quad (6)$$

where H_0 , Ω_M and Ω_Λ denote Hubble constant, matter density parameter today and dark energy density parameter today respectively. The radiation density parameter today Ω_R is omitted here. By Eq. (3) and the observations of GW events, one could estimate the dephasing of GWs. So far aLIGO and AdV's results base on this method is $m_g \leq 7.7 \times 10^{-23}$ eV/c² and $\lambda_g > 1.6 \times 10^{13}$ km [3].

However, in the present work, we consider a new situation in which the orbits of binaries have large eccentricities. Therefore, the GW modes with different frequencies are emitted at the same time from this kind of eccentric sources [20]. In this case, $\Delta t_e = 0$ and Eq. (3) turns into the form

$$\Delta t_a = (1 + Z) \frac{cD}{2\lambda_g^2} \left(\frac{1}{f_e^2} - \frac{1}{f_e'^2} \right). \quad (7)$$

As mentioned above, the eccentricity usually could be ignored at the detectable stage of a comparable mass-ratio binary due to the circularization of the radiation reaction. However, for the large mass-ratio cases, i.e., the EMRIs and IMRIs, the residual eccentricities could still be large at the final stage of inspirals[11]. Thus, eccentric EMRI/IMRI systems will

emit GWs with varied modes of frequencies at the same moment[21]. In other words, if GWs are dispersive, gravitons that emitted at the same moment would also disperse for eccentric binary systems.

The orbits of the small bodies of EMRIs and IMRIs could be complicated. For simplicity, we consider the situation that the eccentric orbit of the small body is set to the equatorial plane of the central body. We use the numerical frame [22] that combines the effective one-body (EOB) dynamics [23] with the frequency-domain Teukolsky equation [24], in which the gravitational waveform could be written as

$$h_+ - ih_\times = \frac{2}{r} \sum_{lmk} H_{lmk} e^{-i\omega_{mk}t + im\phi}, \quad (8)$$

where l, m, k are the harmonic numbers. H_{lmk} describe the amplitude of GWs and could be calculated by the Teukolsky equation, ϕ is the initial phase of GWs, and ω_{mk} is

$$\omega_{mk} = m\Omega_\phi + k\Omega_r, \quad (9)$$

where Ω_r and Ω_ϕ denote the angular frequencies of radial direction and the azimuthal angle respectively. In the following cases, we set $\phi = 0$ for the convenience, and we take the most dominant waves for which $l = m = 2$. In a certain orbital eccentricity e , the amplitudes of modes H_{lmk} depend on the harmonic number k [21]. The frequency of each mode emitted from such eccentric system is $f_e = \omega_{mk}/2\pi$.

Based on above discussions, we calculate some values of Δt_a in different orbital eccentricities for different total masses of system M . In this Letter, we use the cosmological-parameter values of WMAP(Wilkinson Microwave Anisotropy Probe) in nine-year observations[25], i.e. $H_0 = 69.3$ (km/s)/Mpc, $\Omega_M = 0.286$ and $\Omega_\Lambda = 0.714$, and in the following discussion we use this configuration to calculate D and Z from D_L . The maximum mode (where $k = \tilde{k}$) is chosen as the reference point, then the modes with higher ($k > \tilde{k}$) or lower ($k < \tilde{k}$) frequencies have faster or slower speed compared to the \tilde{k} mode. Due to the different speed of modes, after a long distance propagation, the time delay of these modes may be obvious for observation. Some results of Δt_a are shown in Table I and Table II for $e = 0.5$ and $e = 0.7$ respectively, and the semi-latus rectum $p = 12 M$ (in the units with $G = c = 1$, the same as follows). Notice that the delays of arrival time Δt_a of different modes of GWs increase with M . The higher mass corresponding to lower frequency GWs, and by Eq. (7) we know that a lower f_e leads to a larger Δt_a . If the sources located at 1 Gpc, we could see for the

$10^5 M_\odot$ and $10^6 M_\odot$ systems, the time delay of gravitons are from a few hours to more than 10 days, which should be observed easily by the space-based detectors.

TABLE I. The delay of arrival time of GW modes (in seconds) refers the $k = 4$ mode. We set $D_L = 1.00$ Gpc, where $Z \approx 0.20$ and $D \approx 0.83$ Gpc. The Compton wavelength of graviton $\lambda_g = 1.6 \times 10^{13}$ km. The parameters $e = 0.5$, $p = 12 M$, $a = 0.9$, the total masses are $M = 500 M_\odot$, $10^4 M_\odot$, $10^5 M_\odot$, and $10^6 M_\odot$ with the symmetric mass ratio $\nu = 10^{-2}$, 10^{-3} , 10^{-4} , and 10^{-5} respectively.

	k = 2	k = 3	k = 4	k = 5	k = 6
$500 M_\odot$	6.5845×10^{-1}	2.3996×10^{-1}	0	-1.5022×10^{-1}	-2.5046×10^{-1}
$10^4 M_\odot$	2.6341×10^2	9.6016×10^1	0	-6.0126×10^1	-1.0025×10^2
$10^5 M_\odot$	2.6328×10^4	9.5977×10^3	0	-6.0107×10^3	-1.0022×10^4
$10^6 M_\odot$	2.6330×10^6	9.5982×10^5	0	-6.0110×10^5	-1.0023×10^6

TABLE II. The delay of arrival time of GW modes (in seconds) refers the $k = 4$ mode. We set $D_L = 1.00$ Gpc, where $Z \approx 0.20$ and $D \approx 0.83$ Gpc. The Compton wavelength of graviton $\lambda_g = 1.6 \times 10^{13}$ km. The parameters $e = 0.7$, $p = 12 M$, $a = 0.9$, the total masses are $M = 500 M_\odot$, $10^4 M_\odot$, $10^5 M_\odot$, and $10^6 M_\odot$ with the symmetric mass ratio $\nu = 10^{-2}$, 10^{-3} , 10^{-4} , and 10^{-5} respectively.

	k = 8	k = 9	k = 10	k = 11	k = 12
$500 M_\odot$	1.9265×10^{-1}	8.3765×10^{-2}	0	-6.5818×10^{-2}	-1.1847×10^{-1}
$10^4 M_\odot$	7.7072×10^1	3.3514×10^1	0	-2.6336×10^1	-4.7406×10^1
$10^5 M_\odot$	7.7100×10^3	3.3526×10^3	0	-2.6345×10^3	-4.7422×10^3
$10^6 M_\odot$	7.7103×10^5	3.3527×10^5	0	-2.6345×10^5	-4.7423×10^5

As we mentioned before, for GWs with dispersion effect, the dephasing will appear compared to the one without dispersion. In other words, waveforms are distorted by the dispersion during propagation. Fig. 1 shows the distortion of GWs during propagation for $M = 10^6 M_\odot$ case. The length of GW series is 10^4 s without orbital evolution. The strain of GWs here are normalized, so that we could compare the waveforms of GWs in different D_L . It is clear that the waveform is distorted by dispersion effect during the propagation.

Obviously, the time delay will induce dephasing. In Fig. 2, we plot the phase evolution of two waveforms with and without dispersion. It is shown that the dispersion effect has changed the phase of GWs. The dephasing $\Delta\phi$ is the phase difference between the dispersion waveform and the non-dispersive one, and exceeds 1 radian in short duration. Considering LISA is very sensitive to the waveform dephasing, the different of two waveforms should be recognized easily.

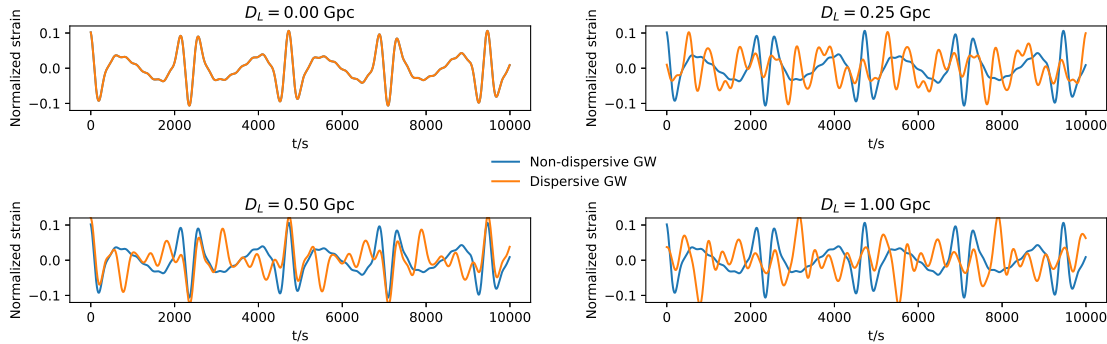


FIG. 1. The distortion of gravitational waves form an extreme-mass-ratio inspiral(EMRI) during propagation. The total Mass $M = 10^6 M_\odot$, the symmetric mass ratio $\nu = 10^{-5}$, $e = 0.5$, $p = 12M$ and $a = 0.9$. We set the luminosity distance of sources D_L from 0 to 1.00 Gpc, and the Compton wavelength of graviton $\lambda_g = 1.6 \times 10^{13}$ km. The orange curves represent the waveforms in dispersion during the propagation, and the cyan one is the non-dispersive ones.

For further discussion of the quantified difference between dispersive GW and non-dispersive GWs, we adopt the well-known matched-filtering technology [26]. Given time series $h_1(t)$ and $h_2(t)$, the overlap or fitting factors of the two series is

$$\text{FF} = \frac{\langle h_1, h_2 \rangle}{\sqrt{\langle h_1, h_1 \rangle \langle h_2, h_2 \rangle}}, \quad (10)$$

where $\langle h_1, h_2 \rangle$ is the symmetric inner product and it has the form

$$\langle h_1, h_2 \rangle = \int_{-\infty}^{\infty} df \frac{\tilde{h}_1(f) \tilde{h}_2^*(f)}{S_n(|f|)}, \quad (11)$$

where the overhead tildes denotes the Fourier transform and the asterisk denotes complex conjugation. $S_n(|f|)$ is the spectral noise density curve, and in this work we use an analytic approximation [27] to the spectral noise density curve of LISA and the zero-detuning high

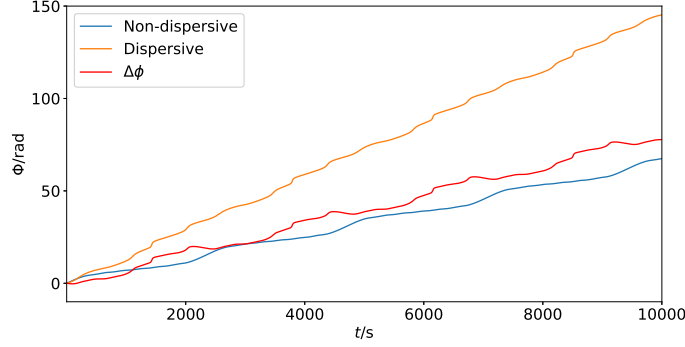


FIG. 2. The phase of gravitational waves in the dispersive case and non-dispersive case and dephasing between two waveforms. The total Mass $M = 10^6 M_\odot$, the symmetric mass ratio $\nu = 10^{-5}$, $e = 0.5$, $p = 12M$ and $a = 0.9$. We set $D_L = 1.00$ Gpc, where $Z \approx 0.20$ and $D \approx 0.83$ Gpc. The Compton wavelength of graviton $\lambda_g = 1.6 \times 10^{13}$ km. The cyan, orange and red curves represent the non-dispersive's, dispersion's phase and dephasing respectively.

power aLIGO configuration[28]. The higher the fitting factor, the more similar the two time series are. For two same time series, the fitting factor is equal to 1. In this Letter, we use fitting factor to quantify the overlap between the GW series with and without dispersion. If the fitting factor is less than 0.97, then we think the two GW series could be distinguished by space-borne detectors.

Results and discussions. We calculate the fitting factors between the dispersive and non-dispersive GW series from eccentric sources, by which we acquire the constraint on λ_g . The length of GW series we discuss below is 17542 M (in the units with $G = c = 1$) without orbital evolution, which equals to one day in $M = 10^6 M_\odot$ case. The fitting factors in different λ_g , M and e are shown in Fig. 3(where $e = 0.5$) and Fig. 4(where $e = 0.7$). Here we define $\lambda_{g0} = 1.6 \times 10^{13}$ km. As is illustrated in the two figures, for inspirals with $M = 500 M_\odot$, the fitting factor is greater than 0.97 all the time. While for inspirals with $M = 10^4 M_\odot$, $M = 10^5 M_\odot$ and $M = 10^6 M_\odot$, the fitting factors vibrate greatly at first (but not greater than 0.97), then increase gradually from 0 around to 1. Especially for $M = 10^6 M_\odot$ case, the fitting factor increase to 1 when $\lambda_g \approx 3 \times 10^3 \lambda_{g0} = 4.8 \times 10^{16}$ km. In future, the space-borne detectors could test this and may give the constraint $\lambda_g > 4.8 \times 10^{16}$ km and $m_g \leq 2.6 \times 10^{-26}$ eV/c². This will be three order better than the current result from LIGO

observations.

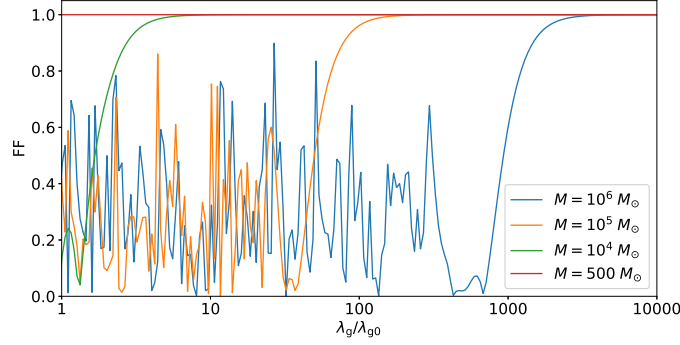


FIG. 3. Fitting factors between dispersive and non-dispersive GW series in different λ_g and M . The unit of λ_g is $\lambda_{g0} = 1.6 \times 10^{13}$ km, the total masses of systems $M = 500 M_\odot$ (red line), $10^4 M_\odot$ (green line), $10^5 M_\odot$ (orange line) and $10^6 M_\odot$ (cyan line), where the symmetric mass ratio $\nu = 10^{-2}$, 10^{-3} , 10^{-4} and 10^{-5} respectively, $e = 0.5$, $p = 12M$ and $a = 0.9$. We set $D_L = 1.00$ Gpc, where $Z \approx 0.20$ and $D \approx 0.83$ Gpc.

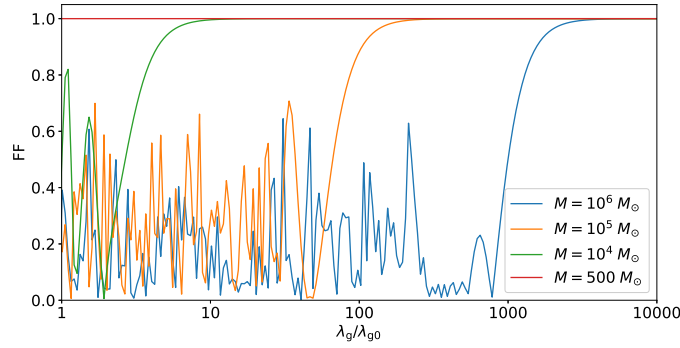


FIG. 4. Fitting factors between dispersive and non-dispersive GW series in different λ_g and M . The unit of λ_g is $\lambda_{g0} = 1.6 \times 10^{13}$ km, the total masses of systems $M = 500 M_\odot$ (red line), $10^4 M_\odot$ (green line), $10^5 M_\odot$ (orange line) and $10^6 M_\odot$ (cyan line), where the symmetric mass ratio $\nu = 10^{-2}$, 10^{-3} , 10^{-4} and 10^{-5} respectively, $e = 0.7$, $p = 12M$ and $a = 0.9$. We set $D_L = 1.00$ Gpc, where $Z \approx 0.20$ and $D \approx 0.83$ Gpc.

The fitting factors in different λ_g and D_L is shown in Fig. 5. Here we set $M = 10^6 M_\odot$. For $\lambda_g = 1.6 \times 10^{17}$ km case, the fitting factor is greater than 0.97 all the time. While for

inspirals with $\lambda_g = 1.6 \times 10^{16}$ km, $\lambda_g = 1.6 \times 10^{15}$ km and $\lambda_g = 1.6 \times 10^{13}$ km, the fitting factors decrease gradually from 1 around to 0 around at first, then vibrate greatly (but not greater than 0.97). Therefore, Fig. 5 could give D_L a lower limits in different λ_g . One certain λ_g limit would not be reached if the D_L below the corresponding lower limit of D_L . For $\lambda_g = 1.6 \times 10^{13}$ km case, the lower limit of D_L may less than 0.1 Mpc. For $\lambda_g = 1.6 \times 10^{16}$ km case, the lower limit of D_L is 0.1 Gpc around.

In one sentence, if observing an eccentric EMRI source with mass around $10^6 M_\odot$ and distance $\gtrsim 0.1$ Gpc, the constraint on graviton mass will be improved about 3 orders compared to the current LIGO results.

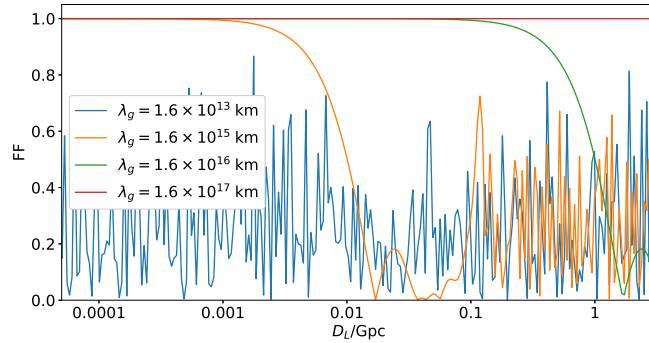


FIG. 5. Fitting factors between dispersive and non-dispersive GW series in different λ_g and D_L . We set the Compton wavelength of graviton $\lambda_g = 1.6 \times 10^{13}$ km (cyan line), 1.6×10^{15} km (orange line), 1.6×10^{16} km (green line) and 1.6×10^{17} km (red line). The total masses of systems $M = 10^6 M_\odot$, the symmetric mass ratio $\nu = 10^{-5}$, $e = 0.5$, $p = 12M$ and $a = 0.9$. We set $D_L = 1.00$ Gpc, where $Z \approx 0.20$ and $D \approx 0.83$ Gpc.

Providing the dispersion effect is significant in the gravitational waveforms, one may doubt that if the dispersive GW series would be matched by a non-dispersive mimic with the only difference in parameters. In other words, if one could distinguish the non-dispersive GW series from a set of the template of the non-dispersive GWs. Thus, we calculate the fitting factors of numerous dispersive GW series and non-dispersive GW templates, and one result is shown in Fig. 6, in which we calculate the fitting factors between a given dispersive GW series and non-dispersive GW series in different e and p . The highest fitting factor is less than 0.35 in this parameter space, and no exception is found yet in other calculations

of us. Therefore, we speculate that we could distinguish the non-dispersive GW series from the templates of the non-dispersive GWs.

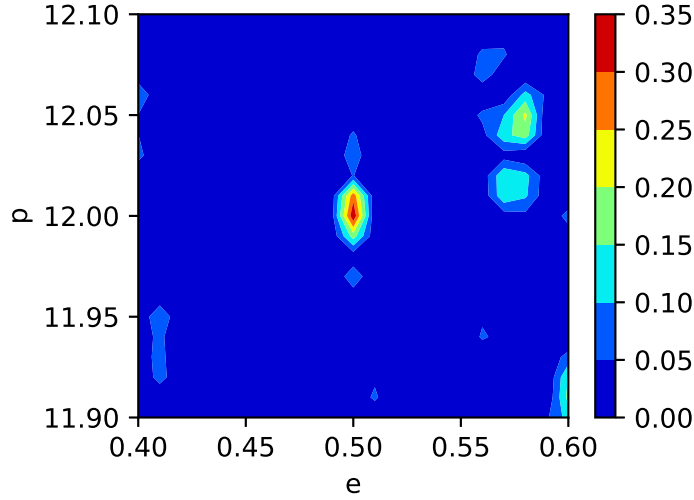


FIG. 6. Contour of fitting factors between dispersive GW series and non-dispersive GW series in different e and p . The dispersive GW series is in $e = 0.5$ and $p = 12M$. Other parameters are the same, the total mass of system $M = 10^6 M_\odot$, the symmetric mass ratio $\nu = 10^{-5}$, $a = 0.9$. We set the luminosity distance $D_L = 1.00$ Gpc, where $Z \approx 0.20$ and $D \approx 0.83$ Gpc, the Compton wavelength of graviton $\lambda_g = 1.6 \times 10^{13}$ km.

To conclude, in this Letter we demonstrate the great potential of EMRI/IMRI signals on the test of GW dispersion, which should be an important scientific target for space-based detectors. We impose the dispersion effect to the gravitational waveforms of EMRIs/IMRIs for which the orbital eccentricities could still be large at the final stage of evolution. The eccentricities lead to varied GW modes to be emitted at the same moment, but arrive at different moments. We demonstrate that the GW dispersion of eccentric sources will cause obvious dephasing and distortion of the waveforms, which could be observed by space-based detectors. Our results show that the observations of EMRIs/IMRIs with LISA will constrain the Compton wave length of graviton λ_g much better than the current level from LIGO observations. In addition, we also investigate this dispersion effect for IMRIs in LIGO

band, and unfortunately aLIGO now may not be able to detect this effect.

- [1] B. P. Abbott *et al.* (LIGO Scientific Collaboration and Virgo Collaboration), Phys. Rev. Lett. **116**, 061102 (2016).
- [2] B. P. Abbott *et al.* (LIGO Scientific Collaboration and Virgo Collaboration), Phys. Rev. Lett. **116**, 241103 (2016).
- [3] B. P. Abbott *et al.* (LIGO Scientific Collaboration and Virgo Collaboration), Phys. Rev. Lett. **118**, 221101 (2017).
- [4] B. P. Abbott *et al.* (LIGO Scientific Collaboration and Virgo Collaboration), Astrophys. J. Lett. **851**, L35 (2017).
- [5] B. P. Abbott *et al.* (LIGO Scientific Collaboration and Virgo Collaboration), Phys. Rev. Lett. **119**, 141101 (2017).
- [6] B. P. Abbott *et al.* (LIGO Scientific Collaboration and Virgo Collaboration), Phys. Rev. Lett. **119**, 161101 (2017).
- [7] G. Amelino-Camelia, SIGMA **2**, 230 (2010).
- [8] A. S. Sefiedgar, K. Nozari, and H. R. Sepangi, Phys. Lett. B **696**, 119 (2011).
- [9] P. Hořava, Phys. Rev. D **79**, 084008 (2009).
- [10] R. Garattini and G. Mandanici, Phys. Rev. D **83**, 084021 (2011).
- [11] P. Amaro-Seoane, J. R. Gair, M. Freitag, M. C. Miller, I. Mandel, C. J. Cutler, and S. Babak, Class. Quantum Grav. **24**, R113 (2007).
- [12] K. Danzmann, L. S. Team, *et al.*, Class. Quantum Grav. **13**, A247 (1996).
- [13] W.-R. Hu and Y.-L. Wu, Natl. Sci. Rev. **4**, 685 (2017).
- [14] J. Luo, L.-S. Chen, H.-Z. Duan, Y.-G. Gong, S. Hu, J. Ji, Q. Liu, J. Mei, V. Milyukov, M. Sazhin, *et al.*, Class. Quantum Grav. **33**, 035010 (2016).
- [15] S. Mirshekari, N. Yunes, and C. M. Will, Phys. Rev. D **85**, 024041 (2012).
- [16] B. P. Abbott *et al.*, Astrophys. J. Lett. **848**, L12 (2017).
- [17] B. P. Abbott *et al.*, Astrophys. J. Lett. **848**, L13 (2017).
- [18] C. M. Will, Phys. Rev. D **57**, 2061 (1998).
- [19] A. G. Riess, A. V. Filippenko, P. Challis, A. Clocchiatti, A. Diercks, P. M. Garnavich, R. L. Gilliland, C. J. Hogan, S. Jha, R. P. Kirshner, *et al.*, Astron. J. **116**, 1009 (1998).

- [20] P. Peters and J. Mathews, Phys. Rev. **131**, 435 (1963).
- [21] W.-B. Han, Z. Cao, and Y.-M. Hu, Class. Quantum Grav. **34**, 225010 (2017).
- [22] W.-B. Han, Int. J. Mod. Phys. D **23**, 1450064 (2014).
- [23] A. Buonanno and T. Damour, Phys. Rev. D **59**, 084006 (1999).
- [24] S. A. Teukolsky, Astrophys. J. **185**, 635 (1973).
- [25] G. Hinshaw, D. Larson, E. Komatsu, D. Spergel, C. Bennett, J. Dunkley, M. Nolte, M. Halpern, R. Hill, N. Odegard, *et al.*, Astrophys. J. Suppl. S. **208**, 19 (2013).
- [26] L. S. Finn, Phys. Rev. D **46**, 5236 (1992).
- [27] S. Babak, H. Fang, J. R. Gair, K. Glampedakis, and S. A. Hughes, Phys. Rev. D **75**, 024005 (2007).
- [28] D. Shoemaker, LIGO Report No. LIGO-T0900288-v3, (2010), the high-power detuned model used in this paper is given in the data file ZERO_DET_HIGH_P.TXT.